Journal of Solid Mechanics Vol. 2, No. 2 (2010) pp. 168-178

Magneto-Thermo-Elastic Stresses and Perturbation of the Magnetic Field Vector in an EGM Rotating Disk

A. Ghorbanpour Arani [1,*], M. Azamia[1], H. Sepiani[2]

[1]*Department of Mechanical Engineering, Faculty of Engineering, University of Kashan, Kashan, Iran*
[2]*Department of Mechanical Engineering, Faculty of Engineering, University of Tehran, Tehran, Iran*

Received 17 May 2010; accepted 20 July 2010

ABSTRACT
In this article, the magneto-thermo-elastic problem of exponentially graded material (EGM) hollow rotating disk placed in uniform magnetic and temperature fields is considered. Exact solutions for stresses and perturbations of the magnetic field vector in EGM hollow rotating disk are determined using the infinitesimal theory of magneto-thermo-elasticity under plane stress. The material properties, except Poisson's ratio, are assumed to depend on variable of the radius and they are expressed as exponential functions of radius. The direct method is used to solve the heat conduction and Hyper-geometric functions are employed to solve Navier equation. The temperature, displacement, and stress fields and the perturbation of the magnetic field vector are determined and compared with those of the homogeneous case. Hence, the effect of in-homogeneity on the stresses and the perturbation of magnetic field vector distribution are demonstrated. The results of this study are applicable for designing optimum EGM hollow rotating disk.

Keywords: EGM; Magneto-thermo-elastic; Rotating disk; Perturbation of magnetic field vector

1 INTRODUCTION

IN 1984, a group of material scientist in Japan introduced the concept of functionally graded material (FGM). An FGM is usually a combination of two material phases that has an intentional graded transition from one material at one surface to another material at the opposite surface. This transition allows the creation of multiple properties (or functions) without any mechanically weak junction or interface. Ceramics and metal are examples of these different materials. Here, the metal is used as a mechanical support structure and the ceramic -because of its low thermal conductivity coefficient and high resistant at high temperature- is used as coating for resisting the high temperature. If pure metals are in those environments, creep and large deformation in structure would be inevitable due to high temperatures. It is possible with these materials to obtain a combination of properties that cannot be achieved in conventional monolithic materials. This makes FGMs suitable for many applications such as the nuclear reactors and high-speed space craft industries.

Up to now, there have only been a few studies on the magneto-thermo-elastic behavior of FGMs. Suresh and Mortensen [1] have provided an introduction to the fundamentals of FGMs. Lutz and Zimmerman [2, 3] obtained analytical solutions for the stresses in spheres and cylinders made of FGMs. Obata and Noda [4] studied the thermal stresses in a functionally graded circular hollow cylinder and a hollow sphere using the perturbation method assuming one-dimensional steady-state conditions. Using the infinitesimal theory of elasticity, Eslami et al. [5] obtained closed-form solutions for stress and displacement in a functionally graded thick sphere subjected to thermal and mechanical loads. Dai and Fu [6] considered the magneto-thermo-elastic problem of FGM hollow structures

* Corresponding author. Tel.: +98 9131626594; fax: +98 361 559930.
E-mail address: aghorban@kashanu.ac.ir; a_ghorbanpour@yahoo.com (A. Ghorbanpour Arani).

subjected to mechanical loads. They assumed that the material properties obey the simple power-law variation through the structures' wall thickness. Naghdabadi and Hosseini Kordkheili [7] have derived thermo-elastic analysis of a FG rotating disk. They obtained a semi-analytical thermoelasticity solution for hollow and solid rotating axsisymmetric disk made of FGMs. Ghorbanpour et al. [8] presented an analytical method to obtain the response of magneto-thermo-elastic stress and perturbation of the magnetic field vector for a thick-walled spherical vessel made of functionally graded materials. The vessel, which was placed in a uniform magnetic field, was subjected to an internal pressure and a transient temperature gradient. They studied the effect of magnetic field vector and material in-homogeneity on the stresses in EGM hollow sphere. Ghorbanpour et al. [9] presented a closed-form solution for one-dimensional magneto-thermo-elastic problem in a FGM hollow sphere placed in uniform magnetic and temperature fields subjected to an internal pressure using the infinitesimal theory of magneto-thermo-elasticity. The results of their study are applicable for designing optimum EGM hollow spheres. Khoshgoftar et al. [10] presented the thermo-piezoelectric behavior of a thick-walled cylinder with functionally graded materials. The cylinder is loaded under the temperature gradient and inner and outer pressures. The main result of their study is that, by applying a proper distribution of mechanical and thermal properties in the functionally graded piezoelectric material (FGPM) solid structures, the distributions of stresses, electric potential and electric field in the FGPM can be controlled. However, exact solution for a hollow rotating disk made of FGM with material properties obeying the exponential variation and placed in uniform magnetic and temperature fields remains to be found.

In this article, exact solutions for the stresses, displacement and perturbation of the magnetic field vector in a hollow rotating disk made of EGM are obtained using the infinitesimal theory of magneto-thermo-elasticity. The properties of the disk, except Poisson's ratio, are assumed to obey exponential variation on the radius. The objective of the present study is to investigate the effect of material in-homogeneity on the magneto-thermo-elastic stresses and perturbation of the magnetic field vector and, thereby, to be able to design optimum hollow disks made of EGM.

2 HEAT CONDUCTION PROBLEM

The disk's material is graded through the r-direction. Thus, the material properties are functions of r. The first law of thermodynamics for energy equation in the steady-state condition without energy generation for an axisymmetric EG one-dimensional disk is given by

$$\frac{1}{r}\frac{\partial}{\partial r}\left(rk(r)\frac{\partial}{\partial r}T(r)\right)=0 \tag{1}$$

It is assumed that the non-homogeneous thermal conductivity $k(r)$ is an exponential function of the radius.

$$k(r)=\overline{k}e^{K\left(\frac{r-a}{b-a}\right)} \tag{2}$$

where $\overline{k}$ in the above relation is the nominal thermal conductivity coefficient and K is in-homogeneity material parameters. Substituting Eq. (2) into Eq.(1) and solving the resulting equation, yields

$$T(r)=D_1\int_a^r\frac{e^{-k(\frac{r-a}{b-a})}}{r}\mathrm{d}r+D_2 \tag{3}$$

where D_1 and D_2 are obtained from the thermal boundary conditions

$$\begin{aligned}&A_{11}T'(a)+A_{12}T(a)=f_1\\&A_{21}T'(b)+A_{22}T(b)=f_1\end{aligned} \tag{4}$$

where $(')$ denotes differentiation with respect to r and $A_{ij}(i,j=1,2)$ are either designate the thermal conductivity or the heat transfer coefficient depending on the type of thermal boundary conditions employed. The constants f_1

and f_2 have known values on the inner and outer radius, respectively. Substituting Eq.(4) into Eq.(3), yields

$$D_1 = \frac{A_{12} f_2 - A_{22} f_1}{(A_{21}\frac{e^{-K}}{b} + A_{22}\int_a^b \frac{e^{-K\left(\frac{r-a}{b-a}\right)}}{r}\mathrm{d}r)A_{12} - \frac{A_{11}}{a}A_{22}}$$

$$D_2 = \frac{(A_{21}\frac{e^{-K}}{b} + A_{22}\int_a^b \frac{e^{-K(\frac{r-a}{b-a})}}{r}\mathrm{d}r) f_1 - \frac{A_{11}}{a} f_2}{(A_{21}\frac{e^{-K}}{b} + A_{22}\int_a^b \frac{e^{-K(\frac{r-a}{b-a})}}{r}\mathrm{d}r)A_{12} - \frac{A_{11}}{a}A_{22}} \tag{5}$$

3 BASIC FORMULATIONS

Consider a thin hollow axisymmetric EG disk with perfect conductivity and a constant thickness, inner and outer radii a and b, respectively, as shown in Fig. 1. This disk placed in a uniform magnetic field $\vec{H}(0,0,H_z)$ and rotating with an angular velocity ω. The disk is thin and the plane stress condition is assumed. Moreover, cylindrical coordinate system (r,θ,z) are used and axial symmetry is assumed.

For the axisymmetric plane stress problem, the constitutive relations are

$$\sigma_r = c_{11}\frac{\partial u}{\partial r} + c_{12}\frac{u}{r} - \lambda_1 T, \qquad \sigma_\theta = c_{12}\frac{\partial u}{\partial r} + c_{11}\frac{u}{r} - \lambda_2 T \tag{6}$$

$$\lambda_1 = c_{11}\alpha_r + c_{12}\alpha_\theta, \qquad \lambda_2 = c_{12}\alpha_r + c_{11}\alpha_\theta \tag{7}$$

where c_{11} and c_{12} are elastic constants, α_r and α_θ are the thermal expansion coefficients, σ_r and σ_θ are the stress components. Assuming that the magnetic permeability μ at the outer surface of the EGM disk to be equal to the magnetic permeability of the medium around it, the medium to be non-ferromagnetic and non-ferroelectric, and omitting displacement electric currents, the governing electro-dynamic Maxwell equations for a perfectly conducting elastic body can be written as [11, 12]

$$\vec{J} = \nabla\times\vec{h}, \qquad \nabla\times\vec{e} = -\mu(r)\frac{\partial\vec{h}}{\partial t}, \qquad div\vec{h} = 0,$$
$$\vec{e} = -\mu(r)(\frac{\partial\vec{U}}{\partial t}\times\vec{H}), \qquad \vec{h} = \nabla\times(\vec{U}\times\vec{H}) \tag{8}$$

Applying an initial magnetic field vector $\vec{H}(0,0,H_z)$ in the cylindrical coordinates (r,θ,z) to Eq. (8), yields

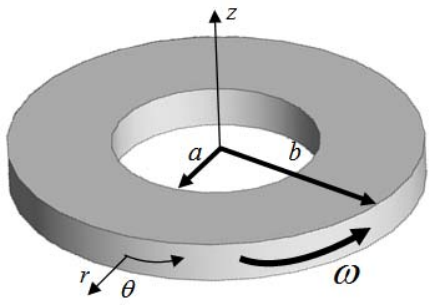

Fig. 1
Configuration of thin-walled finitely radius of the EGM hollow rotating disk.

$$\vec{U}=(u,0,0), \qquad \vec{e}=-\mu(r)(0,H_z\frac{\partial u}{\partial t},0)$$
$$\vec{h}=(0,0,h_z), \qquad \vec{J}=(0,-\frac{\partial h_z}{\partial r},0), \qquad h_z=-H_z(\frac{\partial u}{\partial r}+\frac{u}{r}) \tag{9}$$

The equilibrium equation of the FG rotating disk in the absence of body force is expressed as

$$\frac{\partial \sigma_r}{\partial r}+\frac{\sigma_r-\sigma_\theta}{r}+f_z+\rho r\omega^2=0 \tag{10}$$

where f_z is the Lorentz's force [11, 12] which can be expressed

$$f_z=\mu(r)(\vec{J}\times\vec{H})=\mu(r)H_z^2\frac{\partial}{\partial r}\left(\frac{\partial u}{\partial r}+\frac{u}{r}\right) \tag{11}$$

It is now considered that all material coefficients obey the exponential variation on the radius

$$c_{11}=\overline{c}_{11}e^{K\left(\frac{r-a}{b-a}\right)}, \qquad c_{12}=\overline{c}_{12}e^{K\left(\frac{r-a}{b-a}\right)}, \qquad \alpha_r=\overline{\alpha}_r e^{K\left(\frac{r-a}{b-a}\right)}, \qquad \alpha_\theta=\overline{\alpha}_\theta e^{K\left(\frac{r-a}{b-a}\right)}$$
$$\lambda_1=\overline{\lambda}_1 e^{2K\left(\frac{r-a}{b-a}\right)}, \qquad \lambda_2=\overline{\lambda}_2 e^{2K\left(\frac{r-a}{b-a}\right)}, \qquad \mu(r)=\overline{\mu}e^{K\left(\frac{r-a}{b-a}\right)}, \qquad \rho(r)=\overline{\rho}e^{K\left(\frac{r-a}{b-a}\right)} \tag{12}$$

Here, $\overline{\alpha}_r$, $\overline{\alpha}_\theta$, $\overline{\rho}$, $\overline{\mu}$, $\overline{c}_{11}$ and $\overline{c}_{12}$ are constant and K is in-homogeneity material parameter. $\overline{c}_{11}$ and $\overline{c}_{12}$ for plane stress are given by

$$\overline{c}_{11}=\frac{\overline{E}}{1-\upsilon^2}, \qquad \overline{c}_{12}=\frac{\overline{E}\upsilon}{1-\upsilon^2} \tag{13}$$

where $\overline{E}$ is the elasticity modulus and υ is Poisson's ratio. $\overline{\lambda}_1$ and $\overline{\lambda}_2$ from Eqs. (7) and (12) are given by

$$\overline{\lambda}_1=\overline{c}_{11}\overline{\alpha}_r+\overline{c}_{12}\overline{\alpha}_\theta, \overline{\lambda}_2=\overline{c}_{12}\overline{\alpha}_r+\overline{c}_{11}\overline{\alpha}_\theta \tag{14}$$

3.1 Solution of the Navier equation

By means of Eqs. (12) and (14), substituting Eqs. (6) and (11) into Eq. (10), and by considering Eqs. (3) and (5), the Navier equation in terms of displacement is written as

$$\frac{\partial^2 u}{\partial r^2}+\left(A_1+\frac{1}{r}\right)\frac{\partial u}{\partial r}+\left(\frac{A_2}{r}-\frac{1}{r^2}\right)u=B_1D_1\frac{1}{r}+\left(B_2+\frac{B_3}{r}\right)e^{K\left(\frac{r-a}{b-a}\right)}T(r)-B_4 r \tag{15}$$

where

$$A_1=\frac{K\overline{c}_{11}}{(b-a)(\overline{c}_{11}+\overline{\mu}H_z^2)}, \qquad A_2=\frac{K\overline{c}_{12}}{(b-a)(\overline{c}_{11}+\overline{\mu}H_z^2)}, \qquad B_1=\frac{\overline{\lambda}_1}{\overline{c}_{11}+\overline{\mu}H_z^2}$$
$$B_2=\frac{2K\overline{\lambda}_1}{(b-a)(\overline{c}_{11}+\overline{\mu}H_z^2)}, \qquad B_3=\frac{\overline{\lambda}_1-\overline{\lambda}_2}{\overline{c}_{11}+\overline{\mu}H_z^2}, \qquad B_4=\frac{\overline{\rho}\omega^2}{\overline{c}_{11}+\overline{\mu}H_z^2} \tag{16}$$

The non-homogeneous term on the right-hand-side of Eq. (15) is denoted by F as follows

$$F(r)=B_1D_1\frac{1}{r}+\left(B_2+\frac{B_3}{r}\right)e^{K\left(\frac{r-a}{b-a}\right)}T(r)-B_4r \tag{17}$$

The general solution of Eq. (15) can be written as

$$u(r)=C_1P(r)+C_2Q(r)+R(r) \tag{18}$$

where C_1 and C_2 are arbitrary integration constants, P and Q are homogeneous solutions, and R is the particular solution. Using the method of variation of parameters, the particular solution is written as

$$R(r)=-P(r)\int_0^r\frac{Q(\xi)F(\xi)}{W(\xi)}\mathrm{d}\xi+Q(r)\int_0^r\frac{P(\xi)F(\xi)}{W(\xi)}\,\mathrm{d}\xi \tag{19}$$

where

$$W(r)=P(r)\frac{\mathrm{d}Q}{\mathrm{d}r}-Q(r)\frac{\mathrm{d}P}{\mathrm{d}r} \tag{20}$$

The non-homogeneous differential equation, Eq. (15), is of confluent hyper-geometric type which may be solved by introducing the transformations $u(r)=ry$ and $x=-A_1r$. Using these transformations, the homogeneous part is transformed into

$$x\frac{\partial^2y}{\partial x^2}+\frac{\partial y}{\partial x}(\beta-x)-\chi y=0 \tag{21}$$

where χ and β are given by

$$\chi=1+\frac{A_2}{A_1}=1+\frac{\overline{c}_{12}}{\overline{c}_{11}},\qquad \beta=3 \tag{22}$$

Equation (21) is a standard confluent hyper-geometric differential equation and its solution is written as [13]

$$y(x)=\hat{C}_1F_c(\chi;\beta;x)+\hat{C}_2x^{1-\beta}F_c(1+\chi-\beta;2-\beta;x) \tag{23}$$

where $F_c(\chi;\beta;x)$ is the confluent hyper-geometric function defined by

$$F_c(\chi;\beta;x)=1+\frac{\chi}{\beta.1!}x+\frac{\chi(\chi+1)}{\beta(\beta+1).2!}x^2+\frac{\chi(\chi+1)(\chi+2)}{\beta(\beta+1)(\beta+2).3!}x^3+\cdots \tag{24}$$

Using $u(r)=ry$ and $x=-A_1r$, finally,the following homogeneous solutions are obtained

$$\begin{aligned}&P(r)=rF_c(\chi;\beta;-A_1r)\\&Q(r)=r^{2-\beta}F_c(1+\chi-\beta;2-\beta;-A_1r)\end{aligned} \tag{25}$$

By the virtue of Eqs. (19) and (25), the following expressions for the stresses and the perturbation of magnetic field vector in the EGM hollow disk are derived

$$\sigma_r(r)=C_1V(r)+C_2H(r)+S(r) \tag{26}$$

$$\sigma_\theta(r) = C_1\overline{V}(r) + C_2\overline{H}(r) + \overline{S}(r) \tag{27}$$

$$h_z(r) = -H_z(C_1(\frac{dP(r)}{dr} + \frac{P(r)}{r}) + C_2(\frac{dQ(r)}{dr} + \frac{Q(r)}{r}) + (\frac{dR(r)}{dr} + \frac{R(r)}{r})) \tag{28}$$

where

$$\begin{aligned}
V(r) &= (\overline{c}_{11}\frac{dP(r)}{dr} + \overline{c}_{12}\frac{P(r)}{r})e^{K\left(\frac{r-a}{b-a}\right)} \\
H(r) &= (\overline{c}_{11}\frac{dQ(r)}{dr} + \overline{c}_{12}\frac{Q(r)}{r})e^{K\left(\frac{r-a}{b-a}\right)} \\
S(r) &= (\overline{c}_{11}\frac{dR(r)}{dr} + \overline{c}_{12}\frac{R(r)}{r} - (\overline{c}_{11}\overline{\alpha}_r + \overline{c}_{12}\overline{\alpha}_\theta)e^{K\left(\frac{r-a}{b-a}\right)}T(r))e^{K\left(\frac{r-a}{b-a}\right)}
\end{aligned} \tag{29}$$

$$\begin{aligned}
\overline{V}(r) &= (\overline{c}_{12}\frac{dP(r)}{dr} + \overline{c}_{11}\frac{P(r)}{r})e^{K\left(\frac{r-a}{b-a}\right)} \\
\overline{H}(r) &= (\overline{c}_{12}\frac{dQ(r)}{dr} + \overline{c}_{11}\frac{Q(r)}{r})e^{K\left(\frac{r-a}{b-a}\right)} \\
\overline{S}(r) &= (\overline{c}_{12}\frac{dR(r)}{dr} + \overline{c}_{11}\frac{R(r)}{r} - (\overline{c}_{12}\overline{\alpha}_r + \overline{c}_{11}\overline{\alpha}_\theta)e^{K\left(\frac{r-a}{b-a}\right)}T(r))e^{K\left(\frac{r-a}{b-a}\right)}
\end{aligned} \tag{30}$$

where C_1 and C_2 are constants obtained from boundary conditions.

3.2 Boundary conditions

The following traction conditions on the inner and outer surfaces of the hollow rotating EG disk free-free must be satisfied

$$\begin{aligned}
\sigma_r &= 0 \quad \text{at} \quad r = a \\
\sigma_r &= 0 \quad \text{at} \quad r = b
\end{aligned} \tag{31}$$

In addition, for a hollow rotating EG disk fixed-free the boundary conditions are

$$\begin{aligned}
u &= 0 \quad \text{at} \quad r = a \\
\sigma_r &= 0 \quad \text{at} \quad r = b
\end{aligned} \tag{32}$$

By substituting Eq. (31) into Eq. (26), the constants C_1 and C_2 for hollow disk free-free are derived as follows

$$\begin{aligned}
C_1 &= \frac{H(a)S(b) - H(b)S(a)}{H(b)V(a) - H(a)V(b)} \\
C_2 &= \frac{V(b)S(a) - V(a)S(b)}{H(b)V(a) - H(a)V(b)}
\end{aligned} \tag{33}$$

By substituting Eqs. (26) and (18) into (32), the constants C_1 and C_2 for hollow disk fixed-free are derived as follows

$$C_1 = \frac{S(b)Q(a) - R(a)H(b)}{P(a)H(b) - V(b)Q(a)}$$
$$C_2 = \frac{R(a)V(b) - S(b)P(a)}{H(b)P(a) - Q(a)V(b)} \tag{34}$$

4 NUMERICAL RESULTS AND DISCUSSION

To conduct the numerical calculation, the material constants $\upsilon = 0.3$, $\bar{E} = 200$ GPa, $\bar{\mu} = 4\pi \times 10^{-7}$ H / m, $\bar{\alpha}_r = 2.0 \times 10^{-5}(1/\mathrm{K})$, $\bar{\alpha}_\theta = 1.0 \times 10^{-5}(1/\mathrm{K})$, $\bar{\rho} = 7860(\mathrm{kg}/\mathrm{m}^3)$ are used for the EGM hollow disk. Following Dai and Fu [6], the magnetic intensity is taken as $H_z = 2.23 \times 10^9 (\mathrm{A}/\mathrm{m})$. The inner and the outer radii of the hollow disk are $a = 0.5$ m and $b = 1$ m, respectively, and the disk rotates with an angular velocity $\omega = 6\pi$ rad / s. The thermal boundary conditions are taken as $T(a) = 40\,^\circ\mathrm{C}$ and $T(b) = 10\,^\circ\mathrm{C}$. The temperature, displacement, magneto-thermo-elastic stresses and perturbation of the magnetic field vector for the EGM hollow rotating disk are normalized to demonstrate the effect of in-homogeneity as below

$$T^*(r) = \frac{T(r)}{T(b)}, \qquad u^*(r) = \frac{u(r)}{b}, \qquad \sigma_r^*(r) = \frac{\sigma_r(r)}{\bar{\rho} b^2 \omega^2 e^k}, \qquad \sigma_\theta^*(r) = \frac{\sigma_\theta(r)}{\bar{\rho} b^2 \omega^2 e^k}, \qquad h_z^*(r) = \frac{h_z(r)}{H_z} \tag{35}$$

For different values of *K*, temperature profile, radial displacement, radial stress, circumferential stress and perturbation of magnetic field vector along the radial direction are plotted in Figs. 2-10 for the two following boundary conditions.

4.1 Hollow disk free-free

Fig. 2 shows the variation of temperature along the radial direction for different values of *K*. It is shown that the radial temperature at the internal and external surfaces of the EG hollow rotating disk satisfy the given boundary conditions for the temperature and it decreases with increasing index *K*. The variations of the radial displacement along the radius for different values *K* are shown in Fig. 3. It is seen from this figure that the maximum displacement occurs at the outer radius. The magnitude of the radial displacement is increased as the index *K* is increased. The radial and circumferential stresses are plotted along the radial direction and shown in Figs. 4 and 5. Fig. 4 depicts the distribution of radial stress along the radius for different values of *K*. The figure shows that the radial stresses at the internal and external surfaces of the EGM hollow disk satisfy the given boundary conditions. It is also seen from this figure that the maximum value of the radial stress decreases with increasing index *K* for $K \leq 0$ and the reverse trend is observed for positive values of *K*.

Fig. 5 shows the variations of circumferential stress along the radius for different values of *K*. It is seen from this figure that for different values of the index *K*, the circumferential stress is decreased as *r* is increased. It is also noted that for different values of *K*, circumferential stresses always attain their maximum values at the inner surface and for the positive values of *K*, the distribution of circumferential stress throughout the radius is nearly linear. It is seen from Figs. 4 and 5 that the non-homogeneity parameter *K* has a major effect on the magneto-thermo-elastic stresses so that a negative *K* yields compressive radial and circumferential stresses in the whole EGM hollow rotating disk while a positive *K* gives the opposite result. As can be seen from Figs 4 and 5, the magnitude of circumferential stress is larger than that of the radial stress with increasing *K* at the same point of the EGM hollow rotating disk.

Fig. 6 shows the distribution of the perturbations of magnetic field vector along the radial direction for different values of *K*. It is seen from this figure that the magnitude of perturbation of magnetic field vector becomes small with increasing *K*.

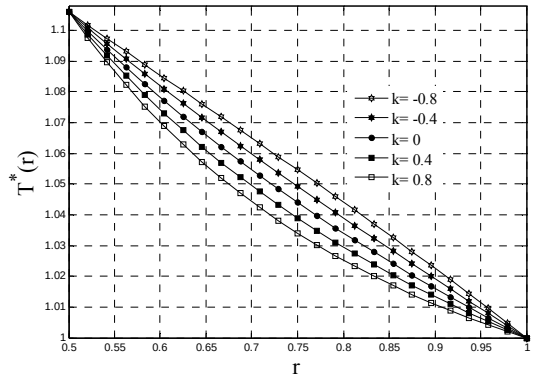

Fig. 2
The radial temperature distribution along the radius in the EGM hollow rotating disk for different values of *K*.

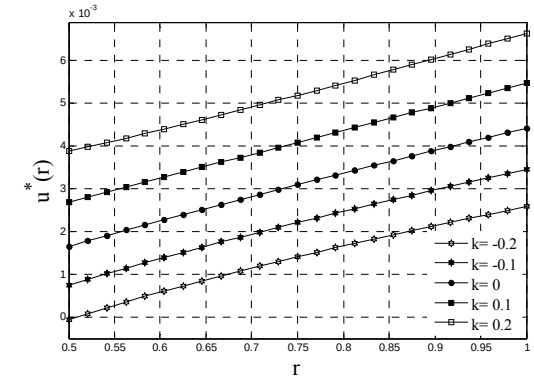

Fig. 3
The radial displacement distribution along the radius in the EGM hollow rotating disk (free-free boundary conditions) for different values of *K*.

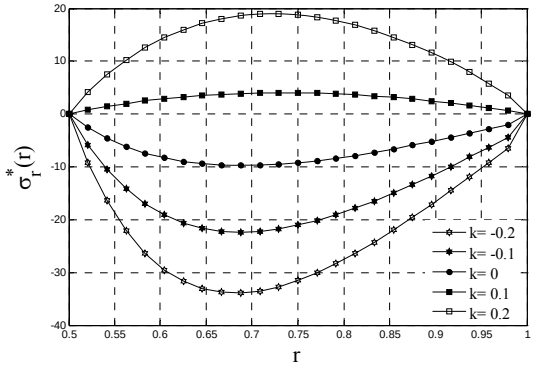

Fig. 4
The radial stress distribution along the radius in the EGM hollow rotating disk (free-free boundary conditions) for different values of *K*.

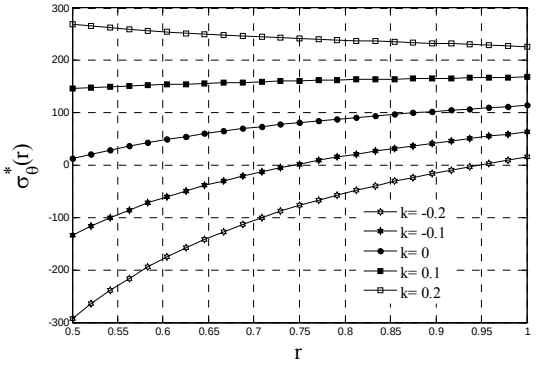

Fig. 5
The circumferential stress distribution along the radius in the EGM hollow rotating disk (free-free boundary conditions) for different values of *K*.

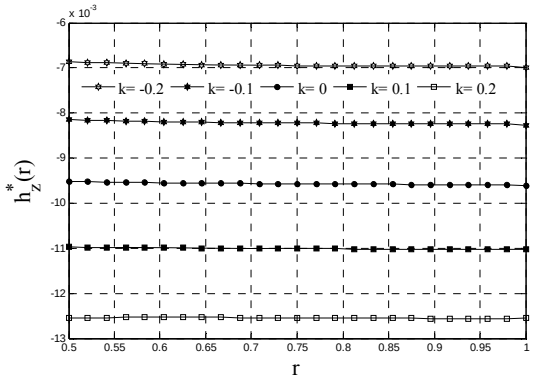

Fig. 6
The perturbation of magnetic field vector along the radius in the EGM hollow rotating disk (free-free boundary conditions) for different values of *K*.

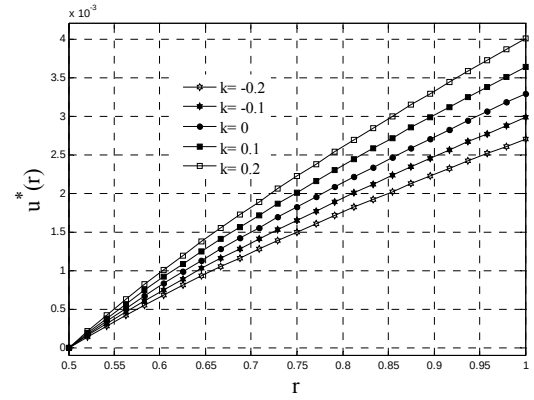

Fig. 7
The radial displacement distribution along the radius in the EGM hollow rotating disk (fixed-free boundary conditions) for different values of *K*.

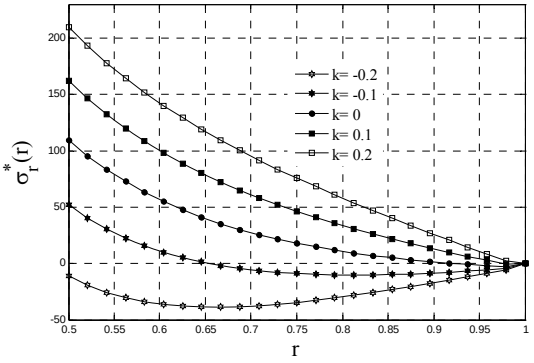

Fig. 8
The radial stress distribution along the radius in the EGM hollow rotating disk (fixed-free boundary conditions) for different values of *K*.

4.2 Hollow disk fixed-free

The variations of the radial displacement along the radius of the EGM hollow rotating disk for different values *K* are demonstrated in Fig. 7. The magnitude of the radial displacement is increased as the power index *K* is increased. It is seen from this figure that the radial displacement satisfies the zero at the internal surface of the EGM hollow rotating disk and the maximum displacement occurs at the outer radius. Fig. 8 shows the distribution of the radial stress along the radius for different values of *K*. It is shown that the radial stress satisfies the zero at the outer radius. As shown in this figure, non-homogeneity parameter *K* as a major effect on the radial magneto-thermo-elastic stresses so that a negative *K* yields compressive radial magneto-thermo-elastic stress distribution along the radius of the disk, while for values nearly $K \geq 0$ gives the contrary result. Fig. 9 shows the distribution of circumferential stress along the radius of the disk for different values of *K*. It is seen easily that the circumferential stress is decreased as the index *K* is increased.

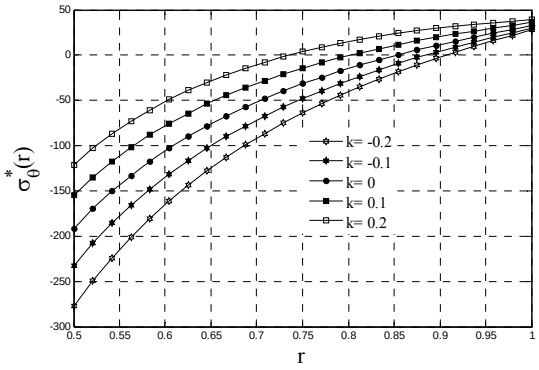

Fig. 9
The circumferential stress distribution along the radius in the EGM hollow rotating disk (fixed-free boundary conditions) for different values of *K*.

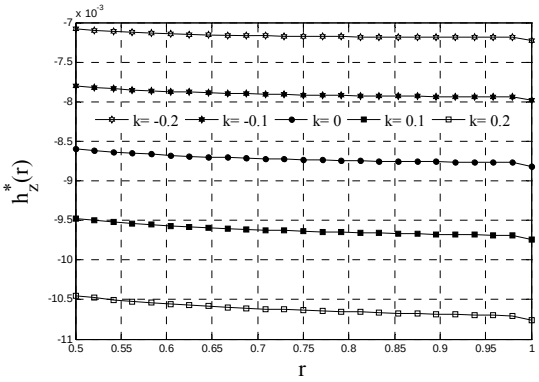

Fig. 10
The perturbation of magnetic field vector along the radius in the EGM hollow rotating disk (fixed-free boundary conditions) for different values of *K*.

The variations of the perturbation of magnetic field vector along the radius of the fixed-free hollow EGM rotating disk for different values of *K* are demonstrated in Fig. 10. This figure shows that the magnitude of perturbation of magnetic field vector becomes small with increasing *K*.

5 CONCLUSIONS

Using the infinitesimal theory of magneto-thermo-elasticity, exact solutions for EGM hollow disks -placed in a uniform magnetic field and temperature gradient- are obtained. The magneto-thermo-elastic stresses are obtained through the direction method of solution of the Navier equation. The material properties through the graded direction are assumed to be nonlinear with an exponential distribution. The results show that the material in-homogeneity has a significant effect on the magneto-thermo-elastic stresses and the perturbation of the magnetic field vector. Moreover, the in-homogeneous constants presented in the present study are useful parameters from a design point of view in that they can be tailored for specific applications to control the distributions of magneto-thermo-elastic stresses. Using the results of this study, it is possible to determine the optimum values for variable *K* in order to have an almost constant circumferential stress with minimal variation along the radial direction. Therefore, the fatigue life of such components can be significantly improved by imposing a magnetic field and optimum values of *K*.

REFERENCES

[1] Suresh S., Mortensen A., 1998, Fundamentals of functionally graded materials, IOM Communications Limited, London, UK.

[2] Lutz M.P., Zimmerman R.W., 1996, Thermal stresses and effective thermal expansion coefficient of a functionally graded sphere, *Journal of Thermal Stresses* **19**:39-54.

[3] Zimmerman R.W., Lutz M.P., 1999, Thermal stresses and effective thermal expansion in an uniformly heated functionally graded cylinder, *Journal of Thermal Stresses* **22**: 177-188.

[4] Obata Y., Noda N., 1994, Steady thermal stresses in a hollow circular cylinder and a hollow sphere of a functionally gradient material, *Journal of Thermal Stresses* **17**: 471-487.
[5] Eslami M.R., Babaei M.H., Poultangari R., 2005, Thermal and mechanical stresses in a functionally graded thick sphere, *International Journal of Pressure Vessels and Piping* **82**: 522-527.
[6] Dai H.L., Fu Y.M., 2007, Magnetothermoelastic interaction in hollow structures of functionally graded material subjected to mechanical loads, *International Journal of Pressure Vessels and Piping* **84**: 132-138.
[7] Hosseini Kordkheili S.A., Naghdabadi R., 2007, Thermoelastic analysis of a functionally graded rotating disk, *Composite Structures* **79**: 508-516.
[8] Ghorbanpour A., Salari M., Khademizadeh H., Arefmanesh A., 2008, Magnetothermoelastic transient response of a functionally graded thick hollow sphere subjected to magnetic and thermoelastic fields, *Archive of Applied Mechanics* **79**: 481-497.
[9] Ghorbanpour A., Salari M., Khademizadeh H., Arefmanesh A., 2010, Magnetothermoelastic stress and perturbation of magnetic field vector in a functionally graded hollow sphere, *Archive of Applied Mechanics* **80**: 189-200.
[10] Khoshgoftar M.J., Ghorbanpour A., Arefi M., 2009, Thermoelastic analysis of a thick walled cylinder made of functionally graded piezoelectric material, *Smart Materials and Structures* **18**: 1-8.
[11] Kraus J.D., 1984, *Electromagnetic*, McGraw-Hill, New York.
[12] Dai H.L., Wang X., 2004, Dynamic responses of piezoelectric hollow cylinders in an axial magnetic field, *International Journal of Solids and Structures* **41**: 5231-5246.
[13] Seaborn J.B., 1991, *Hypergeometric Functions and Their Applications*, Springer, New York.